Monitoring impact damage in composites with large area sensing skins

Vereen, Alexander, Downey, Austin, Sockalingham, Subramani, Ziehl, Paul, LaFlamme, Simon, et al.

Alexander B. Vereen, Austin Downey, Subramani Sockalingham, Paul Ziehl, Simon LaFlamme, Jian Li, Hongki Jo, "Monitoring impact damage in composites with large area sensing skins," Proc. SPIE 11591, Sensors and Smart Structures Technologies for Civil, Mechanical, and Aerospace Systems 2021, 115911Q (22 March 2021); doi: 10.1117/12.2582572

SPIE.

Event: SPIE Smart Structures + Nondestructive Evaluation, 2021, Online Only

Monitoring Impact Damage in Composites with Large Area Sensing Skins

Alexander B Vereen[a], Austin Downey[a,b], Subramani Sockalingam[a], Paul Ziehl[a,b], Simon Laflamme[c], Jian Li[d], and Hongki Jo[e]

[a]Department of Mechanical Engineering, University of South Carolina, Columbia, SC, USA
[b]Department of Civil and Environmental Engineering, University of South Carolina, Columbia SC, USA
[c]Department of Civil, Construction, and Environmental Engineering, Iowa State University, Ames IA, USA
[d]Department of Civil, Environmental, and Architectural Engineering, University of Kansas, Lawrence KS, USA
[e]Department of Civil Engineering and Engineering Mechanics, University of Arizona, Tucson AZ, USA

ABSTRACT

The effect of low energy impacts can seriously impair the operational life span of composites in the field. These low-energy impacts can induce a permanent loss in the toughness of the composite without any visible indication of the material's compromise. The detection of this damage utilizing nondestructive inspection requires dense measurements over much of the surface and has been traditionally achieved by removing the part from service for advanced imaging techniques. While these methods can accurately diagnose the damage inflicted internally by the impacts, they accrue non-trivial opportunity costs while the structure is inspected. To enable the capabilities of in-service monitoring of the composite, the novel soft elastomeric capacitor was investigated as a sensing solution. The sensor is made of three layers comprised of a styrene-ethylene-butylene-styrene (SEBS) matrix, a commercially available elastomer. These layers consist of a titania filled center layer that forms the dielectric of the capacitor and two highly conductive outer layers doped with carbon black. This simple formation allows for a capacitor that has extremely robust mechanical properties. The soft elastomeric capacitor functions by taking up deformations on the surface of the composite that is transduced into a measurable change in capacitance. This study provides an electro-mechanical model for impact damage and experimentally investigates the efficacy of these sensors for use in damage detection given their promising characteristics; that being that the sensor geometry can be arbitrarily large allowing for much fewer sensors than traditional sensor networks employed for this task at a much lower cost than installing traditional in-situ sensing solutions. To investigate these properties a set of impact trials were undertaken on a drop tower using small samples of glass fiber reinforced plate, of random orient and short fiber, with a soft elastomeric capacitor mounted directly opposite the impact site. The impactor head was only allowed one contact with the sample before being intercepted. The testing range for the samples ranged from well below the yield strength of the glass fiber reinforced plate to the ultimate strength of the plate. Experimental results reported a square root relation between the impact energy given to the plate when inducing plastic deformations and the sensor's measured change in capacitance.

Keywords: Soft Elastomeric Capacitor, Structural Health Monitoring, Impact Damage Detection, Sensing Skins, Composite

1. INTRODUCTION

Impact damage detection is a multi-faceted problem in Structural Health Monitoring (SHM) for both the aerospace and civil fields. Methods for impact detection can be separated into global (i.e. modal, harmonic)

Further author information: (Send correspondence to Alexander B Vereen: avereen@email.sc.edu)

Sensors and Smart Structures Technologies for Civil, Mechanical, and Aerospace Systems 2021, edited by Haiying Huang, Daniele Zonta, Zhongqing Su, Proc. of SPIE Vol. 11591, 115911Q
 · doi: 10.1117/12.2582572

and local measurements.[1–3] global methods typically utilize accelerometers to detect structural harmonics while local methods leverage resistive strain gauges (RSG) and PZT to reconstruct a model from key measures of strain.[4–6] The global SHM measures benefit from low labor and cost of implementation when measuring structural disturbances; however, can broadly have trouble with resolution and the particularity of the conclusions that can be drawn.[1,7] Local measurements, in contrast, have less capability informing the overall health of mesoscale structures without impractically large amounts of sensors however where local measurements can be implemented, practical damage detection becomes achievable.[5,8]

The soft elastomeric capacitor (SEC) is a flexible electronic capable of monitoring strain over large areas. SECs function by converting a change in its geometry to a measurable change in capacitance.[9] The sensor is highly elastic and therefore when adhered to a structure deforms with the surface inheriting its surface strains.[9,10] In SHM the strains across the surface are then typically reconstructed to approximate a strain map of the subject using many sensors to best capture features anticipated in the surface.[5] The SEC is an arbitrarily-sized large sensor that gains significant advantages in impact damage detection due to its specific ability to be a large bidirectional sensor.[5,9,10] The SEC is highly elastic, allowing deformations greater than 500%[9] along an axis, and is therefore well-suited for state-based impact detection of composite structures as it can deform during impact without degrading its sensing capability. Moreover, the large area of the SEC allows for sufficient adhesion to the structure which reduced the risk of debonding during impact events.

This work forwards the use of the previously developed SEC for the detection and quantification of impact-induced damage. For impact damage detection, the SEC uses a local state-based measure of strain to detect damage. This method of strain measurement can be leveraged over a large area without an increase of complexity as a single sensor can be manufactured to be many times larger than an RSG. The SEC responds to changes in plate area (i.e. $\varepsilon_x+\varepsilon_y$) and the sum of these strains is demonstrated to be proportional to the strain energy in the sample. This property is shown in this work and supported by experimental observations and mathematically derived for the benefit of clarity. Having a measure proportional to the unit strain energy in a panel can be combined with common failure theories to create clear thresholds to alert of likely part failures in ductile materials beyond the scope of the trials outlined here. To illustrate the sensors' ability for damage detection, an isotropic composite material was chosen to simplify the considerations for modeling the impact. The glass fiber reinforced polyester (GFRP) having a moderate impact resistance was chosen as the sample candidate. The sensors were attached to 150 by 100 mm plates of the composite compliant with ASTM standard D7136M and impacted with a series of impacts of varying energy levels. The energy imparted to the sample is expected to be proportional to the measured change in capacitance.

2. BACKGROUND

The SEC's highly elastic nature means that it is well-suited for impact detection as it is unlikely to produce a hysteric response from strains induced in the material it is monitoring. The sensor is formed from a styrene-ethylene-butylene-styrene (SEBS) matrix with nanomaterials dispersed within its structure. SEBS was chosen as the elastomer for its stability and weather-ability as a matrix for the solute which carries the electrical properties.[9,10] The chosen SEBS compound was shown to exhibit dielectric properties when dispersed with titania.[9] The carbon black material renders the SEB material conductive in contrast. The first step in manufacturing the SEBS is to suspend the elastomer in a compatible solute. Toluene was used to dissolve the SEBS before dispersing the additives into the solution. The next step in manufacturing the SEC is to make the conductive carbon black solution and the dielectric titania solution. This is done using sonication methods to ensure even dispersal of the additives in the solutions.[9]

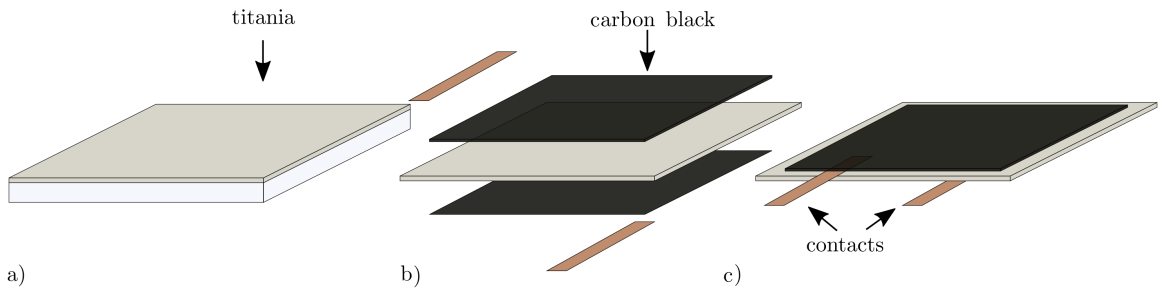

Figure 1. The final steps of manufacturing the SEC: a) drop cast the Titania and SEBS solution evaporating the toluene; b) paint the carbon black and SEBS solution on to the Titania swatch as a thin layer, and; c) place the copper contacts for interacting with DAQ, ensuring to paint over a portion of the copper for good contact.

The dielectric is drop cast onto a glass pane and left to evaporate the excess toluene, as diagrammed in figure 1a). The carbon black SEBS solution is then painted onto the dielectric in progressive layers till a sheet resistivity of less than 1 kΩ is obtained. Two copper tabs are used for metallic connections to connect to the data acquisition system (figure 1c)). These tabs sit on top of a painted layer of carbon black and another layer of the carbon black SEBS solution is then hand-painted on top of the contacts. During manufacturing, square stencils are used to assure the proper dimensioning of the conductive plates. This process achieves a parallel plate capacitor with the mechanical properties of an elastomer. Of key consideration here is the capability of the SEC sensor to deform more than the structure it is attached to without failing before the structure.

3. METHODOLOGY

3.1 Electromechanical Impact Model

A proportional relationship between the strain energy in a material and the measured change in the capacitance of the SEC is derived in this section. From an energy perspective, it can be considered the total energy in an impact is equal to the potential energy minus the non-conservative losses before impact. The bodies during impact store the kinetic energy of the impactor in the GFRP plate. In elastic impacts below the nominal proof resilience, in brittle materials this is the energy required to nearly induce failure, the impactor has its energy restored to the impactor separating the bodies leaving the plate undamaged as shown in Eq. 1. The variables are defined as: E_{sys} = energy present during the impact event, U_{p} = gravitational potential energy, E_{μ} = frictional losses, E_{k} = kinetic energy, and U_{ε} = strain energy and the indices 0 and 1 indicate respectively before or after the impact event in relation to the quantities.

$$E_{\text{sys}} = U_{\text{p0}} - E_{\mu} = E_{\text{k0}} = U_{\varepsilon} = E_{\text{k1}} \tag{1}$$

In a damage event, the material absorbs this kinetic energy storing the energy as strain energy when the nominal proof resilience is exceeded. Modifying Eq. 1 by adding a term to describe retained strain energy within the material $U_{\varepsilon 1}$, Eq. 2 is attained. The retained strain energy $U_{\varepsilon 1}$ will be shown to be proportional to the sensor response.

$$E_{\text{sys}} = U_{\text{p0}} - E_{\mu} = E_{\text{k0}} = U_{\varepsilon 0} = U_{\varepsilon 1} + E_{\text{k1}} \tag{2}$$

The strain taken up by the SEC is a function of the strains at the surface of the GFRP plate. The formulation for strain energy in a plate caused by extensions and contractions in Eq. 5 are derived in the text *Mechanics of fracture initiation and propagation*.[11] Applying the Poisson ratio of the SEC and the identity $\varepsilon_{12} = \frac{\varepsilon_{11}+\varepsilon_{22}}{2}$ to Eq. 3, valid by assuming ε_{11} and ε_{22} to be principal strain directions, where t is the thickness of the plate, and where the area of the GFRP is denoted as A, the Poisson's ratio as ν, and the Young's modulus is denoted as E .

$$U_\varepsilon \approx \frac{Et^3}{12(1-\nu^2)} \cdot A\left(\varepsilon_{11}^2 + \varepsilon_{22}^2\right) \tag{3}$$

$$D = \frac{Et^3}{12(1-\nu^2)} \cdot A \tag{4}$$

$$U_\varepsilon \approx D\left(\varepsilon_{11}^2 + \varepsilon_{22}^2\right) \tag{5}$$

The proposed energy-based modeling spans the impact energy range that results in a purely elastic response to one that produces a small amount of plastic deformation, opposite the impact on the back face of the panel, where the SEC is attached. The transition from a purely elastic response to one that produces plastic deformation happens at the nominal proof resilience or the expected energy to induce failure. By considering impact energy above and below the nominal proof resilience, detection of plastic deformations can be shown. The GFRP composite exhibits desirable behavior due to its largely isotropic behavior. The fiber orientation of the GFRP is random throughout the matrix composed of resin and short fibers, approximating the desired behavior.

The expectation, justified by the model developed here, is that the strain energy present in the material is proportional to the change in capacitance of an SEC attached to the surface. To this point corresponding the changed geometry of an SEC to the change in geometry of the sample it is adhered to is trivial. The SEC is designed to have low stiffness and does not meaningfully resist deformation and therefore inheriting its strains purely from the strain energy stored in the sample. The sensor is also much thinner in comparison to its length and width ensuring the SEC can be assumed to be a thin plate for modeling considerations. Among the advantages yielded by this assumption is that the variation in strain across the SEC will be considered to be negligible as the thickness of the SEC is much less than the arc distance from the center of the material to any point within the SEC. This results in allowing the assumption that the SEC effectively has no thickness and that the strain in the sensor is equal to the strain in the surface to which it is attached. Having established that the sensor is experiencing the strain about the surface of the plate it is bound to, the formulation of the SEC can be forwarded.

$$C = e_0 e_r \frac{A}{d} \tag{6}$$

Eq. 6 is the standard expression for the capacitance of a parallel plate capacitor, which states that the capacitance in a parallel plate capacitor is proportional to the area A of the two parallel plates on to one another divided by the distance between those plates, denoted as d, where the constants of proportionality e_0 denotes the permittivity of free space and e_r denotes the permittivity of the titania filled SEBS.

$$\Delta C = e_0 e_r \left(\frac{A_1}{d_1} - \frac{A_0}{d_0}\right) \tag{7}$$

To normalize this change, Eq. 7 restates the form as the change in capacitance divided by the original capacitance.

$$\frac{\Delta C}{C_0} = \frac{\left(\frac{A_1}{d_1} - \frac{A_0}{d_0}\right)}{\frac{A_0}{d_0}} = \frac{A_1}{d_1}\frac{d_0}{A_0} - 1 \tag{8}$$

Combining Eq. 8 with 9 we retrieve an expression for a normalized change in capacitance as a function of the change in area.[12]

$$\text{Preservation of Mass: } \rho V_1 = \rho V_0 \implies A_1 d_1 = A_0 d_0 \tag{9}$$

$$\frac{\Delta C}{C_0} = \frac{{A_1}^2}{{A_0}^2} - 1 \tag{10}$$

By referencing figure 2 the description of area change as Eq. 11. Using this description, capacitance can be rewritten as a function of plane strains.

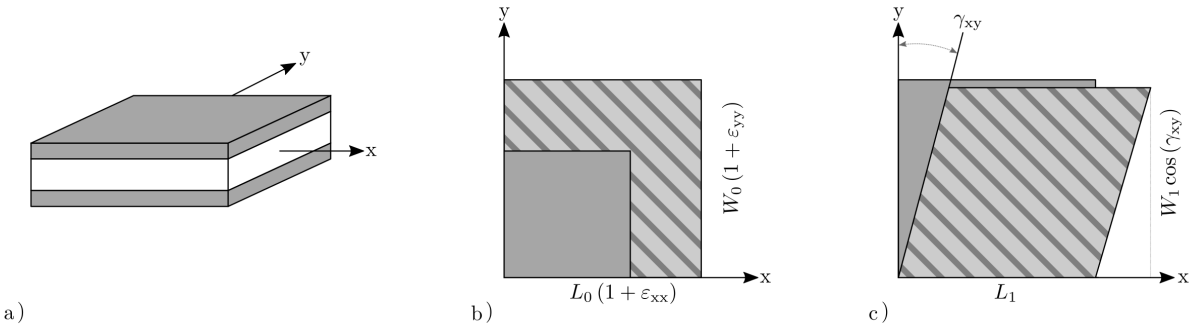

Figure 2. Visualization of the change in area due to plane strains showing: a) a 3D diagram with axes labeled; b) the undeformed shape where L_0 and W_0 are the original length of discrete plane element, and; c) where L_1 and W_1 are the new lengths before shear is accounted for.

$$A_1 = A_0\,(1+\varepsilon_{11})\,(1+\varepsilon_{22})\cos(\gamma_{12}) \approx A_0\,(1+\varepsilon_{11})\,(1+\varepsilon_{22})\left(1-\varepsilon_{12}^2\right) \tag{11}$$

Applying the double angle identity and small-angle approximation of sine, valid for this application due to the small deflections caused by the impact.

$$\frac{\Delta C}{C_0} = (1+\varepsilon_{11})^2\,(1+\varepsilon_{22})^2\left(1-\varepsilon_{12}^2\right)^2 - 1 \tag{12}$$

By removing the orders of strain too high to be significant, namely orders over the first, and assuming the strains to be in principle orientation enables the simplification of Eq. 13.

$$\frac{\Delta C}{C_0} = 2(\varepsilon_{11}+\varepsilon_{22}) \tag{13}$$

Lastly by substituting Eq. 5 into Eq. 13 it can be shown that the sensor functions by a root proportionality to the strain energy within the material.

$$\frac{\Delta C}{C_0} = 2\sqrt{\frac{1}{D}U_\varepsilon} = \mathrm{GF}\cdot\sqrt{U_\varepsilon} \tag{14}$$

Where the gauge factor (GF) can be understood to be $\sqrt{\frac{4}{D}}$ where D is the constant mentioned in Eq.4.

3.2 Experimental validation

To isolate as many factors as possible in analyzing the composites it was decided to use a ASTM D7136M standard drop tower, shown in figure 3a), for impact material properties. The expectation of the glass fibers in the GFRP sample under bending mode is that the material would impose small strains on the sensor before failure due to the impact and larger strains after the nominal proof resilience is exceeded. The material can be expected to respond in three domains: pure elastic responses non-hysteric, small plastic deformations due to its stiffness, and larger deformations post-fracture. The working assumption is made that no strain energy is retained in the material for impacts below the proof resilience of the GFRP panel. Impacts above the proof

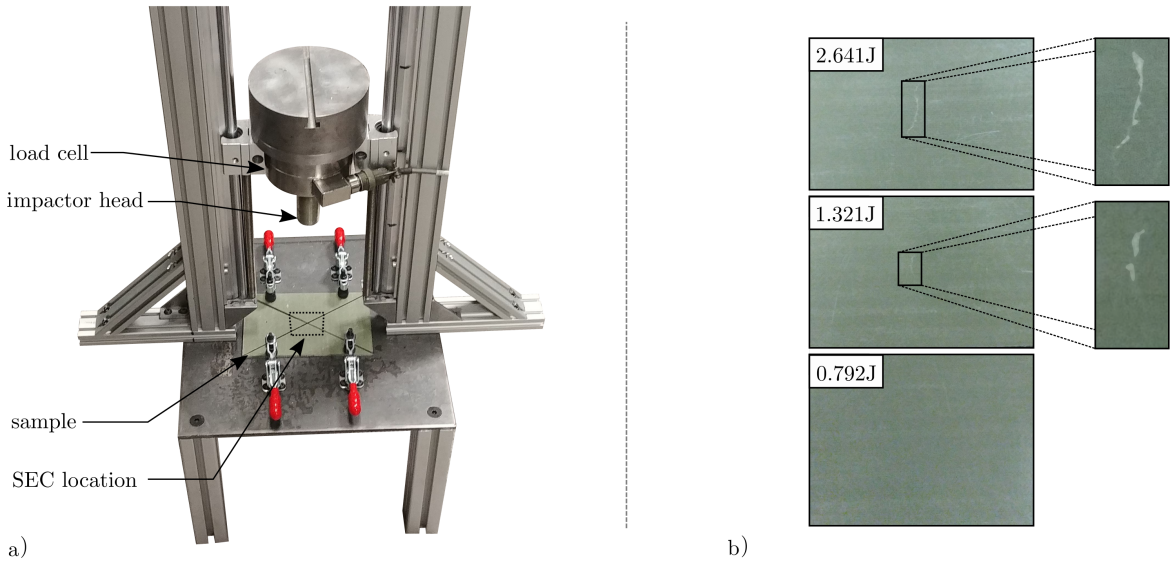

Figure 3. Droptower used for experimental validation showing: a) depiction of the drop tower, and; b) GFRP plates impacted at various drop heights resulting the range of energy shown with the inset highlighting the damage in the plate.

resilience are expected to store energy after the event. These would be registered in the SEC as a sustained increase in capacitance where sub fracture impacts would register no sustained change in capacitance by the SEC (i.e. state-based damage detection).

The impact energy range chosen for this experiment was based on the nominal ratings of the GFRP of 213 $^{J}/_{m}$ to 1,334 $^{J}/_{m}$ and exhibited an expected proof resilience of 0.678 J to 4.237 J for an 3.175 mm GFRP plate. Based on this finding the final range chosen for the trial was a range of drop heights evenly distributed for the impactor head. The range of 0.25 J to 1.5 J impacts was chosen, expressed experimentally as a range of drop heights from 50 mm to 250 mm by 50 mm steps for the drop tower with a 6.5 kg impactor. This made for 5 independent tests on 5 panels of 150 by 100 by 3.175 mm^3 of GFRP.

The goal is to show the transition from the non-destructive elastic impacts to collision events measurable by the sensor where plastic deformations are present. The average measured capacitance before the impact was treated as C_0 and the average capacitance after the collision after the event was taken to be C_1 as unbiased measures of the state over time. The period of the average was considerable to eliminate concerns about signal noise with the average taken for C_0 between the 15 and 2 seconds before the impact and C_1 taken between 2 and 15 seconds after impact. To isolate noise within the capacitance measurements the utmost care was taken to ground all possible sources of interference. The drop tower and impactor head were grounded and tri-axial cabling was used to thoroughly isolate the capacitance measurements. The sample preparation was minimal in line with the advantages of the SEC. No surface preparation was necessary for the GFRP plate before attaching the sensor due to its surface texture. The application of the sensor used a standard epoxy, JB KwikWeld, which was found to work with the sensors agreeably.[5,10] The connections were soldered to the SEC via copper contacts embedded in the sensor during fabrication. The cabling was adhered as close to the SEC as possible to limit the movement during impact or damage to the connection, the former inducing false positive measurements and the latter destroying the equipment. The interface with the contact transitions was firmly secured to avoid jostling, before transitioning to actively shielded triaxial cabling to prevent moving cables from being a source of false signaling due to the impact. Capacitance data was collected using a 40,000 count LCR meter (BK precision 880) with data logged through a LabVIEW VI.

4. RESULTS

Figure 4 reports the forces measured during impact, the measured capacitance, and the change in capacitance following the impact. The impact energy is obtained by taking the integral of the force curve up to its peak

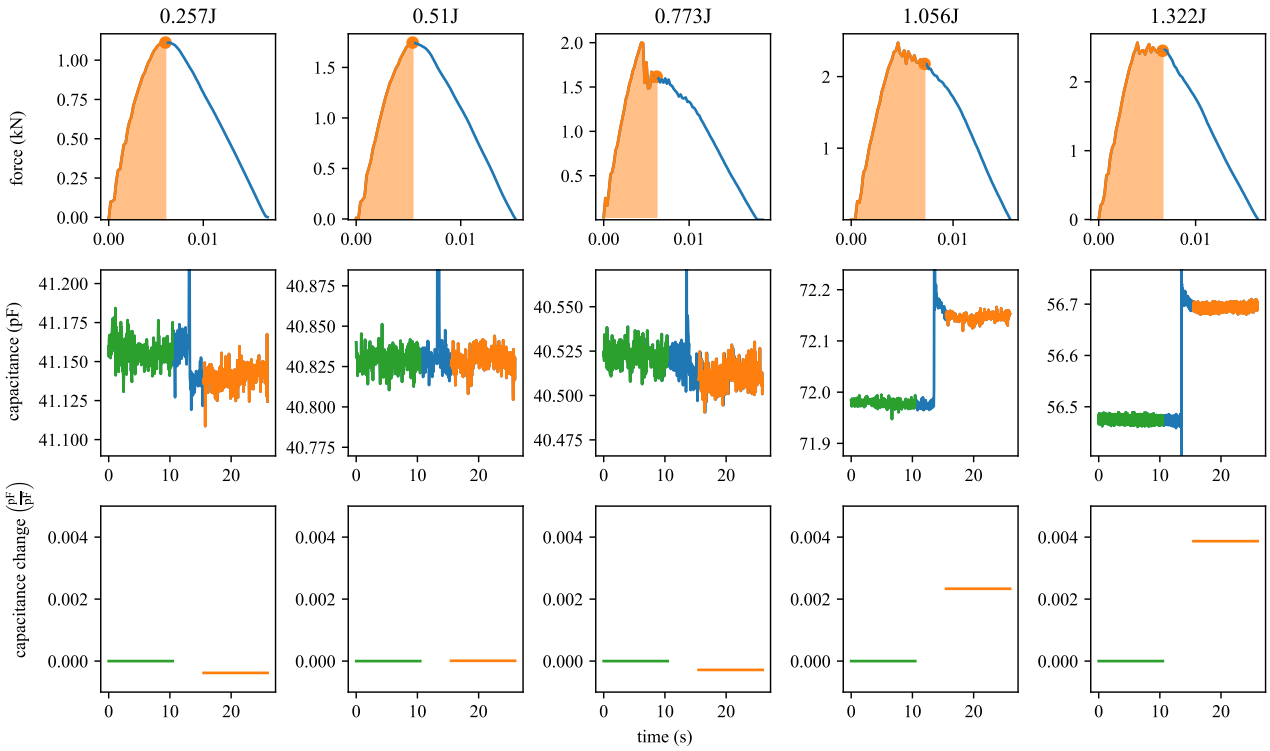

Figure 4. Time-series response for the 5 impacts used in this investigation, showing: (first row) the load cells measure for each individual impact; (second row) the measured capacitance measures and where the data omits the 2 second before and after the impact, and; (third row) the normalized change in capacitance of the region before and after.

as this is where it is assumed the velocity of the impactor goes to zero. From that assumption attaining an approximation of the impact, velocity is trivial. On the second row, the acquired capacitance values are depicted. The capacitance is taken by measuring the average of the two regions before the spike of capacitance caused by the proximity of the metal impactor. The third row of figure 4 depicts the normalized change on capacitance which is shown in Eq. 14 to be proportional to the strain in the plate.

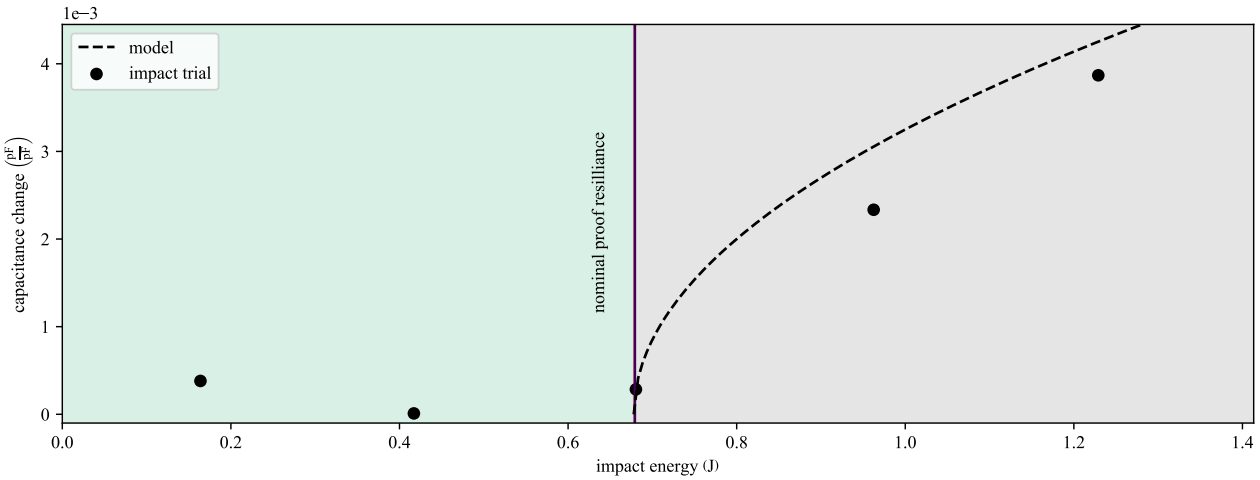

Figure 5. The incurred normalized change in capacitance versus the impact energy as compared to the model.

Figure 5 reports the impact energy versus the normalized capacitance change. The expected capacitance obtained from Eq. 14 is plotted whith a GF= 5.58×10^{-3}, described in Eq. 14, and is compared to the experimental results. The result of the trials was within expectations laid out in experimental validation. The sensor perceived two domains of response. The first domain of response had little to no change in capacitance in the region below the nominal proof resilience. This is the expected response within the elastic range where impacts do not retain strain energy after the event. Exceeding the proof resilience range had marked increases in both visible deformations in the sample, and changes in capacitance seen in figure 5 in line with the expectations laid out in section 3.2.

5. CONCLUSION AND FUTURE WORK

The SEC was investigated as an impact damage detection sensor for composites and presents as a capable tool for practical measurements in that practice. The sensor benefits from being a state-based measurement independent from time allowing for further investigation into the dynamic analysis. The efficacy of the sensor was displayed by an evident change in response corresponding with the initiation of plastic behavior in the GFRP. The analytical form was forwarded as a motivating piece of evidence in the argument for this sensor application. The application of this relation demonstrated the sensor was capable of damage detection, having detected two clear regimes of impacts. Looking to the future, further validation of the model on less brittle material will be undertaken to investigate the sensor behavior and quantify the damage in more ductile materials.

ACKNOWLEDGMENTS

This material is based upon work supported by the National Science Foundation Grant number 1850012 and the Departments of Transportation of Iowa, Kansas, South Carolina, and North Carolina, through the Transportation Pooled Fund Study TPF-5(449). Any opinions, findings, and conclusions or recommendations expressed in this material are those of the authors and do not necessarily reflect the views of the National Science Foundation or the Departments of Transportation of Iowa, Kansas, South Carolina, or North Carolina.

REFERENCES

[1] Gunes, B. and Gunes, O., "Structural health monitoring and damage assessment part i: A critical review of approaches and methods," *International Journal of Physical Sciences* **8**(34), 1694–1702 (2013).

[2] Montazerian, H., Rashidi, A., Milani, A. S., and Hoorfar, M., "Integrated sensors in advanced composites: a critical review," *Critical Reviews in Solid State and Materials Sciences* **45**(3), 187–238 (2020).

[3] Barbosh, M., Singh, P., and Sadhu, A., "Empirical mode decomposition and its variants: a review with applications in structural health monitoring," *Smart Materials and Structures* **29**, 093001 (aug 2020).

[4] Mei, H., Haider, M. F., Joseph, R., Migot, A., and Giurgiutiu, V., "Recent advances in piezoelectric wafer active sensors for structural health monitoring applications," *Sensors* **19**(2), 383 (2019).

[5] Downey, A., Laflamme, S., and Ubertini, F., "Reconstruction of in-plane strain maps using hybrid dense sensor network composed of sensing skin," *Measurement Science and Technology* **27**(12), 124016 (2016).

[6] Sadoughi, M., Downey, A., Yan, J., Hu, C., and Laflamme, S., "Reconstruction of unidirectional strain maps via iterative signal fusion for mesoscale structures monitored by a sensing skin," *Mechanical Systems and Signal Processing* **112**, 401–416 (2018).

[7] Aygun, L. E., Kumar, V., Weaver, C., Gerber, M., Wagner, S., Verma, N., Glisic, B., and Sturm, J. C., "Large-area resistive strain sensing sheet for structural health monitoring," *Sensors* **20**(5) (2020).

[8] Nsengiyumva, W., Zhong, S., Lin, J., Zhang, Q., Zhong, J., and Huang, Y., "Advances, limitations and prospects of nondestructive testing and evaluation of thick composites and sandwich structures: A state-of-the-art review," *Composite Structures* **256**, 112951 (2021).

[9] Laflamme, S., Ubertini, F., Saleem, H., D'Alessandro, A., Downey, A., Ceylan, H., and Materazzi, A. L., "Dynamic characterization of a soft elastomeric capacitor for structural health monitoring," *Journal of Structural Engineering* **141**(8), 04014186 (2015).

[10] Downey, A., Yan, J., Laflamme, S., and Chen, A., "Dynamic reconstruction of in-plane strain maps using a two-dimensional sensing skin," *Structural Health Monitoring 2017* (shm) (2017).

[11] Sih, G., "Strain energy density theory applied to plate-bending and shell problems," in [*Mechanics of fracture initiation and propagation*], 57–98, Springer (1991).

[12] Kong, X., Li, J., Bennett, C., Collins, W., and Laflamme, S., "Numerical simulation and experimental validation of a large-area capacitive strain sensor for fatigue crack monitoring," *Measurement Science and Technology* **27**(12), 124009 (2016).